

Anomalous gauge couplings vis-à-vis $(g - 2)_\mu$ and flavor observables

Debajyoti Choudhury,^{*} Kuldeep Deka,[†] Suvam Maharana,[‡] and Lalit Kumar Saini[§]
Department of Physics & Astrophysics, University of Delhi

We reassess non-standard triple gauge couplings in the light of the recent $(g - 2)_\mu$ measurement at FNAL, the new lattice theory result of $(g - 2)_\mu$ and the updated measurements of several B -decay modes. In the framework of SMEFT, three bosonic dimension-6 operators are invoked to parametrize physics beyond the Standard Model and their contributions to such low-energy observables computed. Constraints on the corresponding Wilson coefficients are then derived from fits to the current experimental bounds on the observables and compared with the most stringent ones available from the 13 TeV LHC data in the W^+W^- and $W^\pm Z$ production channels.

I. INTRODUCTION

Despite its remarkable compatibility with most experimental observations in elementary particle physics, the Standard Model (SM) is plagued by a number of shortcomings warranting explorations in the vistas beyond. While some of the experimental “discrepancies” such as the observation of neutrino masses and mixings are relatively easy to address, others such as anomalies in B -decays, the seeming deviations in the anomalous magnetic moments of the muon and the electron or that in the forward-backward asymmetry in $e^+e^- \rightarrow b\bar{b}$ at the Z -peak have not only been long-standing, but also beg for more complicated solutions.

Solutions to individual issues are, of course, relatively easy to construct, but a coherent explanation is much more difficult to achieve, some recent examples being afforded by efforts that address $(g - 2)_\mu$ in conjunction with discrepancies such as those in low-energy flavour anomalies [1–4], neutrino masses [5–7], dark matter [8–11] and others [12–15]. The difficulty of the exercise can be gauged by the fact that attempted explanations of even a single deviation are constrained by the need to be in accordance with other observables so as to admit only a relatively small parameter space [16–23].

The absence of any new resonances at the LHC strongly suggests that any new physics (NP) explanation of the extant discrepancies would require the operative scale Λ to be at least a few TeVs or larger. Thankfully, even such a little hierarchy between Λ and the electroweak scale validates the use of an effective field theory (EFT) to address these discrepancies [24–27]. While a given ultraviolet-complete theory would yield, on the heavy fields being integrated out, a very specific structure for the ensuing EFT (in other words, specific relations between the Wilson coefficients), in the absence of such a theoretically motivated completion, the coefficients are completely independent. It has to be realized, though, that even apparently independent gauge-invariant opera-

tors may be related through equations of motions and the literature has seen several different choices for the truly independent operators, *viz.* the Warsaw basis [28, 29], the HISZ basis [30], the SILH basis [31] etc. The lack of discernible deviations from the SM expectations have led to constraints on such SMEFT operators, whether of the 4-fermion form [32] or otherwise [27, 33–37]. In this work, we carry on in this spirit, sticking to the HISZ basis.

Of much recent interest has been the Fermi National Accelerator Laboratory (FNAL) measurement [38] of the anomalous magnetic moment of the muon, namely $a_\mu \equiv [(g - 2)/2]_\mu$. The result is consistent with the previous one from the Brookhaven National Laboratory (BNL) measurement, and it is customary to combine the two so as to reduce the experimental errors. As is well-known, a_μ receives many corrections within the SM, of which a particularly difficult calculation is that for the contribution from the hadronic vacuum polarization. The traditional method has been to use dispersion relations alongwith experimental results and if this is adopted, the experimental result would imply a discrepancy $\Delta a_\mu^{\text{DISP}} = 251(59) \times 10^{-11}$, a 4.2σ deviation from the the SM [38, 39]. On the other hand, the adoption of the Lattice QCD results from the Budapest-Marseille-Wuppertal (BMW) collaboration [40] for the same significantly reduces the deviation down to $\Delta a_\mu^{\text{BMW}} = 107(69) \times 10^{-11}$ or an agreement at the 2σ level¹ (see ref [44–46] for reviews).

Also of interest are B physics observables, where neutral current $b \rightarrow sll$ transitions have been showing persistent discrepancy from the SM values in recent years with the most recent result being of the R_K anomaly and $BR(B_s \rightarrow \mu^+\mu^-)$. In Moriond 2021, the LHCb collaboration has reported the measured value of R_K [47] to be $0.846_{-0.041}^{+0.044}$ in the $1.0 \text{ GeV} \leq q^2 \leq 6.0 \text{ GeV}^2$ bin. With the central value remaining virtually unchanged from the earlier result [48], and the errors shrinking by

¹ It should be recognized, though, that while such a positive change in the hadronic vacuum polarization (HVP) minimizes the apparent $(g - 2)_\mu$ discrepancy, it could possibly engender conflicts with the global EW fit prediction of the hadronic contributions to the QED coupling $\Delta\alpha_{\text{had}}^{(5)}$ or elsewhere in low-energy hadron phenomenology [41–43].

^{*} debchou.physics@gmail.com

[†] kuldeepdeka.physics@gmail.com

[‡] smaharana@physics.du.ac.in

[§] sainikrlalit@gmail.com

almost 30%, this has strengthened the deviation from the erstwhile 2.5σ level to 3.1σ . Most interestingly, the value of $BR(B_s \rightarrow \mu^+\mu^-)$ as reported by LHCb is $3.09^{+0.483}_{-0.443} \times 10^{-9}$ [49] and compatible with the SM prediction within 1σ whereas the previous world average (ATLAS, CMS and LHCb) of $2.69^{+0.37}_{-0.35} \times 10^{-9}$ was below the SM prediction by 2σ .

In the present paper, we reexamine possible anomalous self-interactions of the electroweak gauge bosons in the light of these experiments and other such. Concentrating on three particular dimension-6 terms in the SMEFT Lagrangian that lead to anomalous triple gauge boson couplings (TGCs), we evaluate the corresponding one-loop contributions to both $(g-2)_\mu$ and $(g-2)_e$, another observable that shows a discrepancy, albeit smaller as well as certain electroweak precision measurements. While similar exercises have been undertaken in the past [50, 51], our study differs in our inclusion of not only the direct constraints from CMS and ATLAS [52–54], but also the recent results from the LHCb experiment. Assuming that the aforementioned operators are the leading ones, we show that radiative and rare B and K decays such as $B \rightarrow X_s \gamma$, $B_s \rightarrow \mu^+\mu^-$, $B \rightarrow X_s \ell^+\ell^-$, $B \rightarrow K^{(*)}\mu^+\mu^-$, $B_s \rightarrow \phi\mu^+\mu^-$, $K \rightarrow \pi\nu\bar{\nu}$ provide very important constraints. Even though a comprehensive study with the preceding assumption seems quite restrictive at the outset and would, presumably, have very little to say about the mentioned anomalies in terms of a unified explanation, we find that the ensuing results have interesting implications nonetheless, especially with regards to constraining certain classes of new physics models that could potentially serve to explain such discrepancies more efficiently.

This paper is organised as follows. In section II we will introduce the effective Lagrangian for the Electro-Weak (EW) Gauge Bosons and relate the couplings to the Wilson coefficients of the relevant dimension-6 SMEFT operators. In Section III we discuss the anomalous contribution to $(g-2)_\mu$, $b \rightarrow s\gamma$, $b \rightarrow s\mu^+\mu^-$ and $Z \rightarrow b\bar{b}$ using the effective Lagrangian. In Section IV we will present our results using the current experimental observations and also discuss future projections in context of $(g-2)$ experiments. Finally we conclude in Section V.

II. EFFECTIVE LAGRANGIAN FOR THE GAUGE SECTOR

With Λ as the characteristic scale of the UV-complete theory, the EFT operative between the electroweak scale and Λ would be described by a Lagrangian as an expansion in Λ^{-1} with each term being invariant under the full SM gauge group. As the only possible dimension-5 terms do not respect global lepton number, we are eschewing this, and to the leading order, the effective Lagrangian can be expressed as

$$\mathcal{L} = \mathcal{L}_{SM} + \sum_i \frac{c_i}{\Lambda^2} \mathcal{O}_i \quad (1)$$

where \mathcal{L}_{SM} is the SM lagrangian and \mathcal{O}_i is the set of gauge-invariant dimension-6 SMEFT operators with corresponding Wilson coefficients c_i . We make a further assumption that the superheavy fields couple primarily to the bosonic sector and thus the leading corrections are those that involve the latter rather than the SM fermions². The assumption of larger Wilson coefficients for the bosonic operators than those for the 4-fermion operators (despite both sets nominally being of mass-dimension six) may seem an *ad hoc* prescription. However, there exist a plethora of scenarios wherein this could (and is indeed likely to) emerge naturally. Perhaps the most famous of these are Randall-Sundrum-like scenarios with bulk fermions and bosons. The localizations of the light fermions as dictated by the warping, whether a single one [55–57] or a multiple and nested one [58, 59], ensures that the overlap integrals for the KK-gauge bosons with the SM fermions are much smaller than those with the SM bosons. This, immediately, leads to an hierarchy in the Wilson coefficients as examined in this analysis³. Indeed, any model that would include additional particles that couple preferentially to the electroweak bosons rather than to the SM fermions could, in principle, result in larger c_i corresponding to bosonic operators rather than four-fermion operators involving the SM fields alone. Examples are provided by numerous scenarios that contain higher gauge-multiplet fermions such as those in a wide class of scenarios seeking to explain, amongst others, neutrino masses and mixings [60]. In this sense, the analysis presented here serves to assess the viability of such explicit models (many of which, potentially, lead to interesting, albeit complicated signals at the LHC [61, 62]) when juxtaposed with the most recent limits on the low-energy observables, to be described later.

The purely bosonic interactions are expressible in terms of 11 operators[30], of which two ($\mathcal{O}_{\Phi,2}, \mathcal{O}_{\Phi,3}$) contribute, at the tree-level, solely to the Higgs self-interaction. Containing terms proportional to the gauge boson kinetic terms, \mathcal{O}_{BB} and \mathcal{O}_{WW} not only lead to a finite renormalization of the W and B fields respectively, but also contribute to the $H \rightarrow \gamma\gamma/Z\gamma$ decays, and, hence, are constrained by these. Similarly, $\mathcal{O}_{\Phi,1}$ contributes to the Z boson mass but not to the W mass and hence leads to deviations of the ρ parameter from 1. Finally, \mathcal{O}_{DW} and \mathcal{O}_{DB} lead to an anomalous running of the QED fine structure constant and of the weak mixing

² This, of course, is a strong assumption and we would return to this point later.

³ Such a hierarchy would obviously be manifested when the bosonic operators can contribute to an observable at the Born level itself. On the other hand, even when they can contribute only at the loop-level, the hierarchy—itsself depending on the features of the theory such as the extent of warping or the profiles of the low energy fields—can be such that these still overcome the pure-fermionic or mixed fermion-boson operators. We shall implicitly assume this to be so.

angle.

Concentrating, for the sake of simplicity, on only those operators that would leave the largest imprint on the observables of interest, we would examine [30]

$$\begin{aligned}\mathcal{O}_{WWW} &= \text{Tr} \left[\hat{W}_\mu^\nu \hat{W}_\nu^\rho \hat{W}_\rho^\mu \right] \\ \mathcal{O}_W &= (D_\mu \Phi)^\dagger \hat{W}^{\mu\nu} (D_\nu \Phi) \\ \mathcal{O}_B &= (D_\mu \Phi)^\dagger \hat{B}^{\mu\nu} (D_\nu \Phi),\end{aligned}\quad (2)$$

assuming the others to be absent (or, at the least, severely constrained as discussed above). Here, $D_\mu \Phi = \left(\partial_\mu + ig \frac{\sigma_a}{2} W_\mu^a + i \frac{g'}{2} B_\mu \right) \Phi$, $\hat{W}_{\mu\nu} = ig \frac{\sigma_a}{2} W_{\mu\nu}^a$ and $\hat{B}_{\mu\nu} = i \frac{g'}{2} B_{\mu\nu}$. Note that, while analogous CP -odd operators (obtained by replacing a field-strength tensor by its dual) would exist as well, these are irrelevant for our analysis as we deal with only CP -even observables⁴.

The operators in eqn.(2) give rise to, amongst other terms, anomalous triple gauge boson couplings (TGCs). The latter are also often parametrized in terms of a convenient phenomenological Lagrangian [30, 63] namely

$$\begin{aligned}\mathcal{L}_{eff}^{WWV} &= g_{WWV} \left\{ g_1^V \left(\tilde{W}_{\mu\nu}^- \tilde{W}^{+\nu} - \tilde{W}_{\mu\nu}^+ \tilde{W}^{-\nu} \right) V^\mu \right. \\ &\quad \left. + \kappa_V \tilde{W}_\mu^+ \tilde{W}_\nu^- \tilde{V}^{\mu\nu} \right. \\ &\quad \left. + \frac{\lambda_V}{m_W^2} \tilde{W}_\mu^{+\nu} \tilde{W}_\nu^{-\rho} \tilde{V}_\rho^\mu \right\},\end{aligned}\quad (3)$$

with $V \equiv \gamma, Z$. Here, $g_{WW\gamma} = e$, $g_{WWZ} = e \cot \theta$ (with θ being the Weinberg angle) and the field strengths correspond to only the abelian part, $\tilde{W}_{\mu\nu} = \partial_\mu W_\nu - \partial_\nu W_\mu$ and $\tilde{V}_{\mu\nu} = \partial_\mu V_\nu - \partial_\nu V_\mu$. Within the SM, we have $g_1^V = \kappa_V = 1$, $\Delta g_1^\gamma = 0$ and $\lambda_V = 0$. In other words, $\Delta \kappa_V \equiv \kappa_V - 1$, $\Delta g_1^Z \equiv g_1^Z - 1$ and λ_V suitably define the anomalous couplings, and, post symmetry-breaking, can be related to the Wilson coefficients c_W , c_B and c_{WWW} as follows:

$$\begin{aligned}\Delta g_1^Z &= c_W \frac{m_Z^2}{2\Lambda^2} \\ \Delta \kappa_Z &= [c_W - s_\theta^2 (c_W + c_B)] \frac{m_Z^2}{2\Lambda^2} \\ \Delta \kappa_\gamma &= (c_W + c_B) \frac{m_W^2}{2\Lambda^2} \\ \lambda_\gamma &= \lambda_Z = \frac{3m_W^2 g^2}{2\Lambda^2} c_{WWW}.\end{aligned}\quad (4)$$

⁴ The leading contributions of the CP -odd dimension-6 operators to the CP -even observables would appear only at second order in the corresponding Wilson coefficients. In the ensuing analysis, however, we limit contributions only upto a linear order in the WCs. Assuming higher order terms would further require the inclusion of operators of similar mass-dimensions (dimension-8 and higher) in the theory which is beyond the scope our current study.

In the above and in the following sections we use the notation $s_\theta = \sin \theta$ and $c_\theta = \cos \theta$.

Although the operators \mathcal{O}_{DW} and \mathcal{O}_{BW} too contribute to the anomalous triple gauge couplings, their primary effect on low-energy physics accrue through the modification of the gauge boson propagators and, hence, these are not as visible in processes such as W^+W^- production in LEP[64] and LHC experiments.

III. CONTRIBUTIONS TO VARIOUS OBSERVABLES

At this stage, the choice of the gauge is an important one. While full $SU(2) \otimes U(1)$ gauge invariance is manifest in the formulation of eqn.(2), it is not so for the case where eqn.(3) is supposed to encapsulate the entire non-SM part of the effective Lagrangian. In view of this, and for the sake of convenience, we adopt the unitary gauge for all our calculations.

A. a_μ

Starting with the effective Lagrangian as described in the preceding section, we may now compute the contribution to the magnetic moment of the muon. At the one-loop order, the only contributing diagram is as shown in Fig. 1. To this order, then, the only relevant part of the

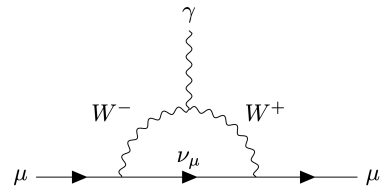


FIG. 1: Diagram contributing to $\Delta a_\mu^{\text{anom}}$ at 1-loop involving an aTGC vertex.

higher-dimensional terms is that subsumed in eqn.(3), and more specifically

$$\mathcal{L}_{\Delta a_\mu} \supset \frac{g}{\sqrt{2}} (\bar{\mu} \gamma^\mu P_L \nu_\mu) W_\mu^- + \text{h.c.} + \mathcal{L}_{\text{eff}}^{WW\gamma}, \quad (5)$$

with P_L being the left-handed projection operator. Since we are dealing with a nonrenormalizable Lagrangian, we expect the integral to be a divergent one (a simple power counting ensuring that it is only a logarithmic divergence), necessitating the introduction of a cutoff. A nat-

ural choice for the latter is Λ itself⁵, leading to

$$\Delta a_\mu^{anom.} = \frac{e^2}{48\pi^2 s_\theta^2} \frac{m_\mu^2}{m_W^2} \left\{ \Delta\kappa_\gamma \left(\frac{1}{3} + \ln \left[\frac{\Lambda^2}{m_W^2} \right] \right) + \lambda_\gamma \left(\frac{7}{6} - \ln \left[\frac{\Lambda^2}{m_W^2} \right] \right) \right\}. \quad (6)$$

where we have retained only terms at the leading order in m_μ^2/m_W^2 and neglected m_ν altogether. This expression can, of course, be trivially translated in terms of c_{WWW} and the combination $(c_W + c_B)$ using eqns.(4). While Fig.1 represents the only one-loop contribution to Δa_μ emanating from the Lagrangian of eqn.(3), when the SMEFT language of eqn.(2) is used instead, additional contributions arise from diagrams with a Higgs in the loop. Contrary to naive expectations, these are *not* small compared to that in eqn.(6). The analytic expressions thereof are more unwieldy though, and, for the sake of brevity we omit presenting those. However, we do include such contributions in our numerical analysis. Note that the four-point (or higher) vertices that eqn.(2) engenders—and not included in eqn.(3)—contribute to a_μ only at the two-loop or higher orders.

In the preceding and subsequent loop calculations we adopt dimensional regularization alongwith the $\overline{\text{MS}}$ renormalization scheme. While it is often argued that the simple pole at $d = 4$ (d being the number of dimensions) could be straightforwardly exchanged for a logarithmic dependence on the cutoff Λ , the said dependence is better understood as a consequence of the renormalization group (RG) evolution of the effective operators from the scale Λ down to the EW scale [65]. Note that we ignore the (subdominant) contributions of terms with higher powers of the logarithm and the EW couplings which appear in perturbative solutions of the RGEs.

It might seem that the contribution \mathcal{O}_{WWW} is in disagreement with the results of ref.[66], which were expressed in terms of the dipole operator. Of particular significance is the presence of the $\ln(\Lambda^2/m_W^2)$ dependence in our result *vis á vis* the apparent absence of c_{WWW} in the anomalous dimension (as computed in the Warsaw basis) of $c_{e\gamma}$ (or, equivalently, c_{eB} and c_{eW}). However, a comparison between operators in different bases needs to be made with care, especially since the dipole operators (*sans* the Higgs field) are admissible only post electroweak symmetry breaking. A careful matching reintroduces this effect, and, indeed our result for Δa_μ is, consistent with that given in ref.[27] obtained from the one-loop matching between LEFT and SMEFT operators at the electroweak scale.

While we have argued for the Wilson coefficient $c_{e\gamma}$ being, at best, tiny at the scale Λ , it is worthwhile to

examine whether it could be amplified at the EW scale as a result of mixing, under RG evolution, with the other operators in the theory. Note that the operators we use are a part of the HISZ set which, in consisting of only eleven purely bosonic operators, does not constitute a closed set under RG evolution. However, confined to this subset, these modulo a difference in the normalizations, can be exactly mapped onto operators in the SILH basis. Inspired by the latter, if we were to augment the set by the inclusion of the dipole operator ($c_{e\gamma}$), its evolution would depend mainly on \mathcal{O}_{BW} ($\equiv H^\dagger H W_{\mu\nu} B^{\mu\nu}$) apart from \mathcal{O}_B and \mathcal{O}_W . The dependence of Δa_μ on the last two operators has already been calculated above to one-loop order and any residual dependence would be further loop-suppressed and negligible. The Wilson coefficient for \mathcal{O}_{BW} , on the other hand, is constrained by the LEP experiments (from oblique corrections) to be tiny [30]. Consequently, any enhancement, on evolving down to the EW scale (or even lower) in such an explicitly introduced $c_{e\gamma}/\Lambda^2$ is tiny. For example, a value of starting with $c_{e\gamma}/\Lambda^2 \sim \mathcal{O}(10^{-3} \text{ TeV}^{-2})$ and $c_{BW}/\Lambda^2 \sim \mathcal{O}(0.1 \text{ TeV}^{-2})$ at $\Lambda = 1 \text{ TeV}$, the RG evolution down to the EW scale results in a change of less than 1% in either. In other words, the running effects can be neglected.

It is easy to see that an expression analogous to that in eqn.(6) would hold for Δa_e with m_μ replaced by m_e . Most importantly, the sign of the new contributions would be identical in the two cases, which is in disagreement with the experimental results.

B. Flavor Observables

The anomalous gauge couplings can also contribute to various loop-mediated flavour changing neutral current hadronic decays. The said decays may occur through a multitude of effective operators such as the electromagnetic dipole or semi-leptonic vector and axial-vector ones, namely

$$\begin{aligned} \mathcal{Q}_7 &= \frac{e}{(4\pi)^2} m_b (\bar{s}_L \sigma_{\alpha\beta} b_R) F^{\alpha\beta} \\ \mathcal{Q}_9 &= \frac{e^2}{(4\pi)^2} (\bar{s}_L \gamma_\alpha b_L) (\bar{l} \gamma^\alpha l) \\ \mathcal{Q}_{10} &= \frac{e^2}{(4\pi)^2} (\bar{s}_L \gamma_\alpha b_L) (\bar{l} \gamma^\alpha \gamma_5 l) \end{aligned} \quad (7)$$

where L and R denote the chirality of the fermionic fields, $\sigma_{\alpha\beta} = i[\gamma_\alpha, \gamma_\beta]/2$ and $F^{\alpha\beta}$ is the electromagnetic field tensor. The $\Delta B, \Delta S = 1$ operator is traditionally written as

$$\mathcal{L} = \frac{4G_F}{\sqrt{2}} (C_7 \mathcal{Q}_7 + C_9 \mathcal{Q}_9 + C_{10} \mathcal{Q}_{10}) + H.c \quad (8)$$

with C_7, C_9 and C_{10} being the corresponding Wilson coefficients that factorise the short distance physics. We have omitted above the right-handed analogues of C_9, C_{10}

⁵ While this identification might seem an *ad hoc* one, note that the cutoff has to be $\lesssim \Lambda$, and given the logarithmic nature of the dependence, a small variation would be numerically insignificant.

as, to the leading order, the operators of interest do not contribute to these. The anomalous contributions appear as a result of the diagrams in Figure 2.

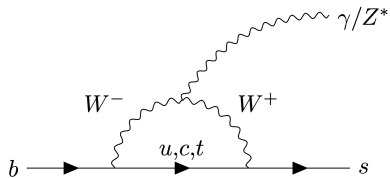


FIG. 2: Diagram contributing to $b \rightarrow s \gamma(Z^*)$ at 1-loop.

Although we use dimensional regularisation, it is instructive to trace the divergences of the 1-loop contributions in generality. The photonic diagram thus generated mirrors that for $\Delta a_\mu^{\text{anom}}$ and is only logarithmically divergent. For the Z vertex, on the other hand, if a momentum cutoff were used instead, the anomalous contribution from an individual quark loop would be found to be quadratically divergent (in dimensional regularisation, this is manifested as a pole at $d = 2$). However, thanks to the GIM mechanism, the quadratically divergent pieces (as with any other term independent of the internal quark mass) cancel, leaving behind only a logarithmic divergence. Of these, the top-quark contribution dominates overwhelmingly [67] and we can fairly approximate ($x \equiv m_t^2/m_W^2$)

$$C_i \approx (C_i)_{SM} + \left[V_{tb} V_{ts}^* \frac{m_W^2}{\Lambda^2} \right] \Delta C_i \quad (9)$$

with

$$\begin{aligned} \Delta C_7 &= \frac{-(c_B + c_W)}{8(x-1)^2} \left[2x + \frac{x^3 - 3x^2}{(x-1)} \ln x \right] \\ &+ \frac{3g^2 c_{WWW}}{8} \left[\frac{x^2 + x}{(x-1)^2} - \frac{2x^2 \ln x}{(x-1)^3} \right], \\ \Delta C_9 &= \left\{ \frac{-(c_B + c_W)}{8} x + \frac{3c_W}{16} \frac{1 - 4s_\theta^2}{s_\theta^2} x \right\} \ln \left(\frac{\Lambda^2}{m_W^2} \right) \\ &+ \frac{3g^2 c_{WWW}}{4(x-1)^2} \left[x - 3x^2 + \frac{2x^3 \ln x}{(x-1)} \right], \\ \Delta C_{10} &= \frac{-3c_W}{16s_\theta^2} x \ln \left(\frac{\Lambda^2}{m_W^2} \right). \end{aligned} \quad (10)$$

The subdominant contributions from the up- and charm-loop can be easily read off. For $b \rightarrow d$ and $s \rightarrow d$ transitions, analogous analyses follow, but with the identity of the dominant loop changing.

C. $Z \rightarrow b\bar{b}$

The presence of the anomalous gauge couplings also leads to a modification in the electroweak precision variables, whether these be the oblique corrections or the

fermion-gauge couplings. Of particular importance is the $Zb\bar{b}$ coupling and the ρ (equivalently, T) parameter. The effective $Zb\bar{b}$ vertex may be parametrized as

$$\mathcal{L}_{Zb\bar{b}} = \frac{e}{s_\theta c_\theta} \left[(g_L^b + \delta g_L^b) \bar{b}_L \not{Z} b_L + (g_R^b + \delta g_R^b) \bar{b}_R \not{Z} b_R \right] \quad (11)$$

where $g_L = (-1/2 + s_\theta^2/3)$ and $g_R = (s_\theta^2/3)$ are the SM values of the couplings. The one-loop contributions of the dimension-6 operators are encapsulated by the two diagrams⁶ of Fig. 3. It should be noted here that, unlike in the previous two cases, an analysis with eqn.(3) is no longer appropriate for it does not possess the full $SU(2) \otimes U(1)$ gauge invariance. With a treatment of the oblique corrections being contingent on this gauge invariance, the use of full eqn.(2) becomes mandatory. With

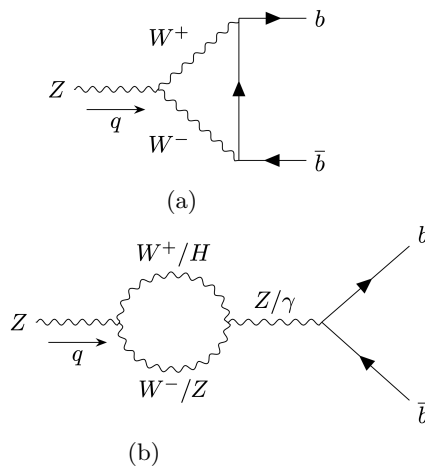


FIG. 3: Diagrams contributing to the $Z \rightarrow b\bar{b}$ decay corresponding to (a) vertex correction and (b) wavefunction renormalisation of Z -boson propagator.

the most sensitive data on $\delta g_{L,R}^b$ being obtained at the Z -pole, it is convenient to separate the corrections into two parts. One of these originates from the wave-function renormalization of the Z boson due to a one-loop oblique

⁶ There is, of course, a diagram analogous to Fig. 3(a), but incorporating the ZZH vertex instead of the ZWW one. However, being suppressed by an extra factor of m_b^2/m_W^2 , the corresponding contribution is negligible in size.

correction Π_{ZZ} (Fig. 3b) and is given by⁷

$$\begin{aligned}
(\delta g_{L,R}^b)_{ob} &= \frac{-\alpha_{em}}{4\pi\Lambda^2} g_{L,R}\mathcal{A} \\
\mathcal{A} &\equiv \frac{gv m_Z}{4c_\theta} \left(\frac{m_H^2}{2m_Z^2} + \frac{2}{3} \right) \left(\frac{c_B}{c_\theta^2} + \frac{c_W}{s_\theta^2} \right) \log \frac{\Lambda^2}{m_H^2} \\
&+ \frac{m_Z^2}{2s_\theta^2} \log \frac{\Lambda^2}{m_W^2} \\
&\times \left(3(1 - 6c_\theta^2)g^2 \frac{m_W^2}{m_Z^2} c_{WWW} + \left[4c_\theta^2 - \frac{5}{6} \right] c_W \right. \\
&\quad \left. - \frac{1 + 4c_\theta^2 - 36c_\theta^4}{12c_\theta^2} [c_\theta^2 c_W - s_\theta^2 c_B] \right)
\end{aligned} \tag{12}$$

The second contribution emanates from the direct one-loop correction to the vertex (Fig 3a). Applicable only to the left-handed coupling⁸, it is given by

$$\begin{aligned}
(\delta g_L^b)_v &= \left[\frac{\alpha_{em} |V_{tb}|^2}{16\pi s_\theta^2} \frac{m_Z^2}{2\Lambda^2} \right] \mathcal{B} \log \frac{\Lambda^2}{m_W^2} \\
\mathcal{B} &\equiv [c_W - s_\theta^2(c_W + c_B)] \left(-1 + \frac{x}{2} - \frac{1}{6} \frac{m_Z^2}{m_W^2} \right) \\
&- c_W c_\theta^2 \left(-\frac{5m_Z^2}{3m_W^2} + 3x \right),
\end{aligned} \tag{13}$$

Tracing the divergences, we again note that, unlike in the preceding cases, the GIM mechanism is not operative here, resulting in quadratic and higher divergences as well. However, following the arguments in refs. [65, 68], we presume that such loop contributions provide the correct dependence on the new physics scale only upto terms scaling logarithmically with Λ and that higher divergences would be cancelled by counter-terms in the EFT. The expressions in eq.(13) differ from those given in ref. [67] by a relative sign between the $\Delta\kappa_Z$ and Δg_1^Z contributions. The oblique correction Π_{ZZ} in eq. (12) matches with that calculated in ref [50] for the WW -loop. Besides, we have also calculated the ZH -loop contribution to the Z -propagator which hasn't been included in ref. [67].

The logarithms in above equations are associated to the RG evolution between Λ and m_W . As argued in ref. [67], since $y_t^2/(4\pi)^2 \ln(\Lambda^2/m_W^2) \ll 1$ (with y_t being the top-quark Yukawa coupling) resumming the corresponding leading-logarithms is not numerically important and retaining only the unresummed $\ln(\Lambda^2/m_W^2)$ contribution, as above, is a very safe approximation.

IV. RESULTS

TGCs have been probed in many collider experiments over the years and deviations from the SM values have been increasingly constrained with an increase in the collision energy. The most recent studies by ATLAS and CMS experiments at the LHC [52–54, 69–71] have primarily analysed multiple production channels such as W^+W^- , $W^\pm\gamma$ and $W^\pm Z$ with the first-mentioned proving to be the most restrictive. Each such underlying process can result in different final states and several have been explored. Of the two most sensitive studies, one [53] considers the W^+W^- channel with both W s decaying leptonically, leading to a $l_a^+ \nu_a l_b^- \bar{\nu}_b$ final state. The major reducible backgrounds emanate from the Drell-Yan production of lepton pairs and $t\bar{t}$ events in which both top quarks decay leptonically. The Drell-Yan events can be suppressed by selecting the two leptons to be of different flavor (one electron and one muon), whereas contributions from $t\bar{t}$ events can be reduced by rejecting events with b-tagged jets. The second important analysis [52] considers both W^+W^- and $W^\pm Z$ production where one W decays leptonically and the other W/Z decays hadronically resulting in a $l^\pm \nu q q'$ final state. In this case, the two major backgrounds are $W + jets$ and $t\bar{t}$, and a major portion can be reduced by using a combination of kinematical cuts and jet substructure techniques. On the other hand, LEP experiments also posit bounds on the same operators from W^+W^- and single W production channels [72]. Of the several studies, the most stringent bounds on the anomalous TGCs, in terms of the Wilson coefficients c_B/Λ^2 , c_W/Λ^2 and c_{WWW}/Λ^2 , have been provided in [52] for the LHC operating $\sqrt{s} = 13$ TeV and we use these for all subsequent comparisons. We note that the one-parameter best fit limits on c_B/Λ^2 and c_W/Λ^2 from Higgs production and decay measurements presented in ref. [73], although stricter, are comparable with those from the TGC measurements. However, we do not refer to these limits in our analysis explicitly as the ensuing sections (IV A–IV C) deal only with two-dimensional parameter spaces in the WCs. In what follows, we compare the current limits from the LHC against those obtained from the aforementioned observables for a benchmark value of the cutoff scale Λ .

A particular point needs to be noted at this juncture. An EFT such as that in eqn.(2) should, ideally, be used in calculating cross sections only when $\sqrt{\hat{s}} \lesssim \Lambda$, where, \hat{s} denotes the partonic center-of-mass energy. In the case of the LHC, this would nominally imply that $\Lambda \gtrsim \mathcal{O}(1 \text{ TeV})$ —even accounting for the nontrivial parton distribution functions—a constraint that is often overlooked in interpreting results, generally presented in terms of c_i/Λ^2 .

In Table I we list the current limits for the aforementioned observables. For the case of $(g-2)_\mu$ we quote two different values for the discrepancy $\Delta a_\mu^{\text{anom.}}$, namely, $\Delta a_\mu^{\text{DISP}}$ (WP20) and $\Delta a_\mu^{\text{BMW}}$ (BMW). The limits on ΔC_9 and ΔC_{10} are derived from single parameter fits to all

⁷ It should be remembered that, in the spirit of EFTs, only terms linear in the Wilson coefficients should be retained.

⁸ There is, indeed, a vertex correction engendered by the anomalous ZZH coupling that contributes to δg_R^b . However, the contribution is suppressed by the bottom mass.

$b \rightarrow sl^+l^-$ branching ratio and angular observables (including that of $\Lambda_b \rightarrow \Lambda\mu^+\mu^-$) excluding⁹ the observables sensitive to lepton flavour universality (LFU) such as the ratios $R_{K^{(*)}}$ [74]. Similar fits have also been performed by other groups, see e.g.[75–77]. On the other hand, the limits on ΔC_7 are extracted from the inclusive B-meson radiative decay ($\mathcal{B}_{s\gamma} : B/\bar{B} \rightarrow X_s\gamma$) observable $R_{X_s} \equiv \mathcal{B}_{s\gamma}/(\mathcal{B}_{s\gamma})_{SM}$ [78, 79]. It is important to note that the exclusion of the observables such as $R_{K^{(*)}}$, is enforced by the fact that whereas their current measurements hint towards a violation of LFU, the operators under discussion are strictly flavour blind.

Current limits	
Observable(\mathcal{F})	1σ limit
$\Delta a_\mu^{\text{DISP}}$ (WP20)	$251 \pm 59 \times 10^{-11}$
$\Delta a_\mu^{\text{BMW}}$ (BMW)	$107 \pm 69 \times 10^{-11}$
ΔC_7	-0.03 ± 0.03
$\Delta C_{9\mu\mu}$	-1.03 ± 0.13
$\Delta C_{10\mu\mu}$	0.41 ± 0.23
ΔC_{9ee}	0.70 ± 0.60
ΔC_{10ee}	-0.50 ± 0.50
δg_L	0.0016 ± 0.0015
δg_R	0.019 ± 0.007

TABLE I: *Current experimental limits on various observables affected by anomalous TGCs*[74, 80].

A. 2σ bands for all observables for current limits

In our quest to study the low-energy constraints in their totality, we begin by studying each in isolation. Assuming, for the purpose of easy visualization, that only the Wilson coefficients c_B, c_W are nonzero, we present, in Fig. 4, the ensuing bounds in this plane emanating from the individual observables in Table I with the assumption that the new physics scale¹⁰ $\Lambda \sim 2$ TeV. Several features are worth noting:

- The Δa_μ -allowed band (purple), as calculated using the WP20 result [39] does not include the SM point, reflecting the fact that the data does not agree with the SM value at the 2σ level. For the lattice result (BMW) [40], though, it is indeed included. For brevity’s sake, here, and in subsequent

⁹ The global fit that we refer to, from [74], does not include the $B_{s,d} \rightarrow \mu^+\mu^-$ branching ratios. Including this, however, would only have a marginal effect on the fit result and, hence, can be safely ignored.

¹⁰ Note that, unlike the collider bounds (which have been derived by neglecting all subleading dependence on Λ), the SMEFT constraints in Fig. 4 have additional logarithmic dependence of Λ , and we would return to this point later.

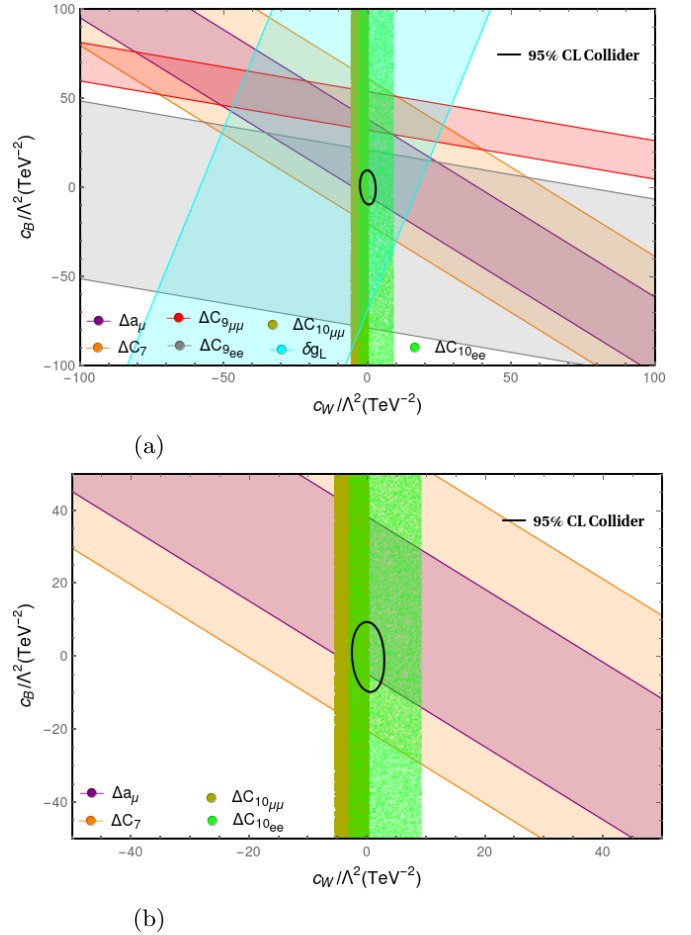


FIG. 4: *The 2σ ranges in the c_W/Λ^2 - c_B/Λ^2 plane allowed by individual observables. $\Lambda = 2$ TeV has been used along with the lattice result [40]. The lower panel shows an enlarged portion of the same. The black ellipse identifies the LHC limit.*

discussions, we display only the figures corresponding to the BMW result, while keeping under consideration the WP20 alternative as well.

- The corresponding band for Δa_e sits on the opposite side of the origin, owing to the sign of the discrepancy. However, with the anomalous contribution being suppressed by m_e^2 , the required sizes of the Wilson coefficients are too large to be meaningful.
- δg_L has a relatively weaker dependence on c_B than on c_W (see eqns.(12&13)) leading to the slightly tilted band. δg_R , on the other hand, receives a small correction only from the correction to the Z self-energy, and the ensuing bounds are too weak to be relevant.
- Since ΔC_7 , just like Δa_μ , parametrizes the coupling of a fermion current to the photon, both are understandably proportional (in the absence of a

nonzero c_{WWW}) to the combination $(c_B + c_W)$ and the ensuing bands are parallel to each other.

- ΔC_{10} , being dependent on c_W alone, leads to a relatively narrow vertical band in this plane. Most restrictive of all the observables, the difference in its value as calculated from the electronic and muonic channels exert opposite pulls leading to the two parallel bands. Although both bands overlap with the collider limit, the one corresponding to the muonic channel has a greater sensitivity to c_W and, hence, its partial overlap presents a comparatively stronger constraint on the allowed region, favouring negative values for c_W .

This leads to an interesting possibility wherein ΔC_{10} is the dominant flavour-blind Wilson coefficient parametrizing new physics effects in FCNC B decays. A sizable range of c_W values compatible with the LHC limits exists that could, then, ameliorate the discrepancies in the aforementioned B decay observables (excluding LFU ones). Not contributing to ΔC_{10} , a similar-sized c_B would lead to only tiny changes in the low-energy observables (see the zoomed-in view of Fig.4b) and would be primarily constrained by collider experiments.

- Similar to the preceding observable, the opposing experimental numbers for ΔC_9 from the two (e and μ) channels lead to two bands.
- It is quite apparent that the flavor observables $\Delta C_{7,9,10}$ give some of the strongest constraints. Indeed, with many of the bands intersecting each other at different angles, it is expected that combining the individual data, when independent, would lead to constraints much stronger than individual ones. Whether such combined constraints agree with the LHC results is an aspect which we address in the following subsection.

Before we attempt this, it behoves us to consider the limits afforded on c_{WWW} and we display these in Fig.5, once in the c_B - c_{WWW} plane (keeping $c_W = 0$) and once in the c_W - c_{WWW} plane (keeping $c_B = 0$). With their dependences on c_{WWW} being different, the bands due to Δa_μ and ΔC_7 are no longer parallel. ΔC_9 continues to be a restrictive force in the c_B - c_{WWW} plane, while its effect is reduced in the c_W - c_{WWW} plane (owing to the smaller dependence on c_B). For δg_L , it is, quite understandably, the other way around.

It needs to be appreciated at this point that the nominal restrictions from the low-energy observables are much weaker than those obtained at the LHC, as exhibited by all the panels of Figs.4&5. This situation changes drastically once we attempt to simultaneously fit all the observables as we see next. Also worth noting is the fact that much of the parameter space satisfying the individual observables fall outside the domain wherein the EFT series expansion can be safely deemed valid and, hence,

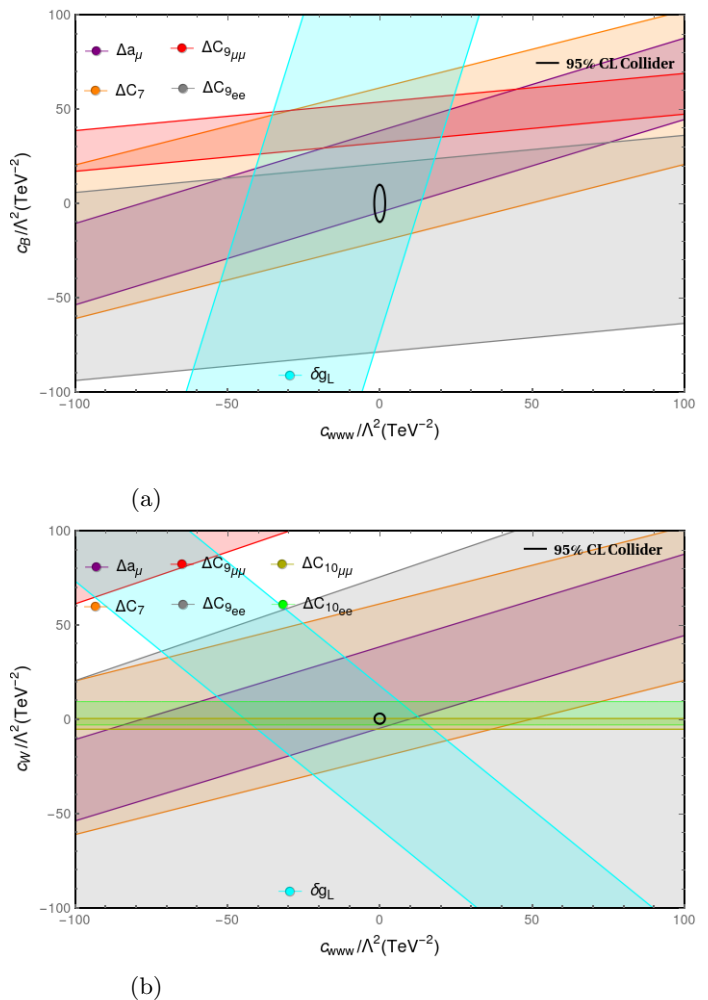


FIG. 5: The 2σ bands as derived from the individual observables from anomalous TGCs considering BMW result [39] as the theory value in the c_{WWW}/Λ^2 - c_B/Λ^2 (upper panel) and c_{WWW}/Λ^2 - c_W/Λ^2 (lower panel) planes along with the 13 TeV experimental constraints.

caution must be exercised while reading off such regions as constraints on the WCs.

B. Fitting all observables

We now perform a combined fit of the non-standard parameters (c_B , c_W , c_{WWW}) to the observables defined in sec.(III). To this end, we define a χ^2 as a function of the anomalous parameters, namely

$$\chi^2(c_B, c_W, c_{WWW}; \Lambda) = \sum_i \left(\frac{\mathcal{F}_i^{\text{exp}} - \mathcal{F}_i^{\text{th}}}{\sigma_i} \right)^2, \quad (14)$$

where i runs through all the observables, $\mathcal{F}_i^{\text{exp}}$ are the experimental values with standard deviations σ_i and $\mathcal{F}_i^{\text{th}}$ denote the corresponding theoretical expectations for a

given set of values for the Wilson coefficients. The best-fit point would then be given by the minimum of the χ^2 and parameter points leading to $\chi^2 \leq \chi^2_{min} + \delta\chi^2$ being inseparable from the best-fit point at a confidence level determined by $\delta\chi^2$. As before, in order to render the constraints more tractable, we consider only two nonzero Wilson coefficients at a time, holding Λ to a fixed value.

The calculation of the χ^2 entails inclusion of either only independent measurements, or if more variables are to be considered, an appropriate inclusion of the correlation matrix. For the sake of simplicity, we adopt the former method despite the attendant loss of sensitivity. This allows us to use the corresponding measurements (alongwith the errorbars) from Table I in a straightforward manner. In particular, thanks to the flavour universal nature of the Wilson coefficients in the theory, we make use of both the muonic ($\Delta C_{\mu\mu}$) as well as the electronic (ΔC_{ee}) limits simultaneously.

Calculation	Descriptor	$(c_B, c_W, c_{WWW})/\Lambda^2$ [TeV ⁻²]	χ^2
WP20	SM	(0,0,0)	101.76
	2-param B.F.	(39.26, -1.64, 0)	25.76
	3-param B.F.	(38.48, -1.63, -2.97)	25.71
BMW	SM	(0,0,0)	86.121
	2-param B.F.	(35.05, -1.83, 0)	28.663
	3-param B.F.	(36.65, -1.85, 6.41)	28.446

TABLE II: Results of the different χ^2 analyses described in the text.

We, thus, have two inequivalent scenarios (depending on whether we choose the WP20 or BMW calculation) that the theory is to be compared with. The resultant χ^2_{min} values are tabulated in Table II. Also tabulated, for comparison, are the χ^2 values for the SM point. The strikingly different χ^2 values for the latter under the two schemes is but a consequence of the difference in the theoretical predictions for $(g-2)_\mu$. Also, note that the rather large values for the SM point are driven, to a large extent, by the flavour universal B -decay observables.

To interpret these results, it is instructive to consider a projection to a two-parameter space, which we consider to be the $(c_W/\Lambda^2, c_B/\Lambda^2)$ plane with c_{WWW} held zero. The corresponding global fit, in the best case scenario (*i.e.*, BMW), is illustrated in Fig.6a wherein we show the best-fit with the attendant 95% C.L. contour. We note that the χ^2 -fit not only prefers the best-fit value to be far away (as determined on the scale of the LHC limits) from the SM value, but even the two 95% ellipses (direct limits and low energy preference) do not overlap with each other. That the separation is larger along the c_B -axis can be understood qualitatively by comparing the individual bands in Fig.4a. On account of the relatively small uncertainty associated with it, the muonic ΔC_9 measurement exerts the strongest pull on c_B , thereby

pulling the best-fit point upward.

As can be gleaned from eq.10, and as has already been reflected in Fig.5, the observables under consideration have only a very weak dependence on c_{WWW} . Consequently, its contribution to the χ^2 is relatively small, and, on its inclusion in the minimization, the erstwhile minimum in the two-parameter fit (with $c_{WWW} = 0$) only expands into a very shallow basin. This is reflected by Table II, where the inclusion of c_{WWW} doesn't have any significant impact on the (c_B, c_W) coordinates of the best-fit point. Similarly, the improvements in the attendant χ^2_{min} values are only marginal.

A caveat needs to be discussed at this point. Although we have been characterizing our fits as functions of c_i/Λ^2 , in actuality we have held Λ to a specific value (2 TeV) especially in the calculation of the logarithms. Increasing it to higher values not only brings the best-fit point closer to the SM, but also, understandably, shrinks the 95% C.L. ellipse significantly (see Fig. 6b). The apparent tension with the LHC constraints is maintained. This disagreement is expected to persist as, with additional luminosity (LHC Run III, HL-LHC, etc.) or higher energies (a future collider or an upgrade of the LHC), the collider limits are likely to shrink too (as it already has for the 13 TeV run as compared to the 8 TeV one[52]).

C. Future Projections

The analysis in the preceding subsection establishes that an effort to explain $(g-2)_\mu$ or several other discrepancies in the low-energy data in terms of anomalous triple-gauge boson couplings (or, equivalently, the corresponding bosonic operators in the SMEFT) would require couplings (Wilson coefficients) that are too large given the LHC constraints. It is, then, of interest to speculate whether near-future improvements in the low-energy data are likely to lead to constraints stronger than those already imposed by the LHC. As a particular example, we choose to do this for $(g-2)_\mu$. With the experiment at FNAL projecting a reduction in the uncertainties by a factor of about four [39], it is worth re-examining our analysis with the following two assumptions as to the tentative outcomes by the end of the FNAL experiment(s):

1. *Reduced uncertainties in Δa_μ with the same central value*

With no significant improvement in the theoretical calculations envisaged in the near future, if the central value of the experimental measurement remains unchanged, we would be likely to face $\Delta a_\mu^{\text{DISP}} = (251 \pm 15) \times 10^{-11}$ ($\Delta a_\mu^{\text{BMW}} = (107 \pm 17.15) \times 10^{-11}$) pertaining to the WP20 (BMW) analyses. The corresponding χ^2 -fit for the projected $\Delta a_\mu^{\text{BMW}}$ (best case scenario) is shown in Fig.7(blue curve). Comparing with the current limits presented in Fig.6a we note that while the best fit point has shifted

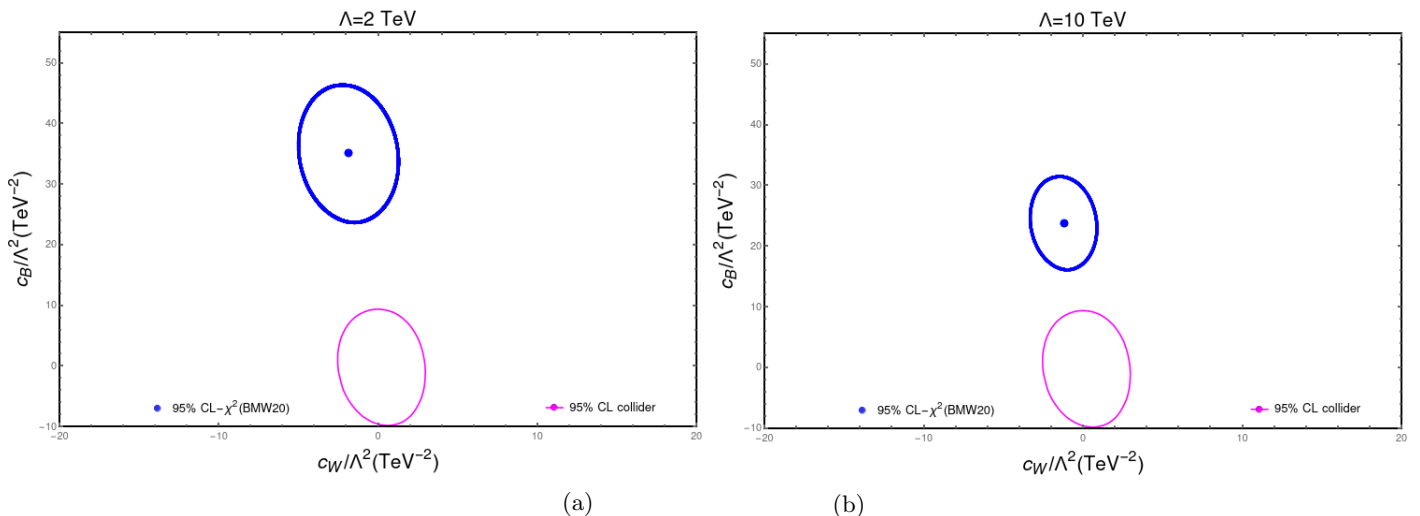


FIG. 6: *6a* shows the result of the χ^2 analysis in the BMW case for $\Lambda = 2$ TeV, and the collider result at 95% confidence level, in the c_W/Λ^2 - c_B/Λ^2 plane. *6b* shows the same for $\Lambda = 10$ TeV.

marginally towards the SM point along the c_B/Λ^2 direction, the corresponding 95% C.L. contour has, expectedly, shrunk. The overall tension would actually increase.

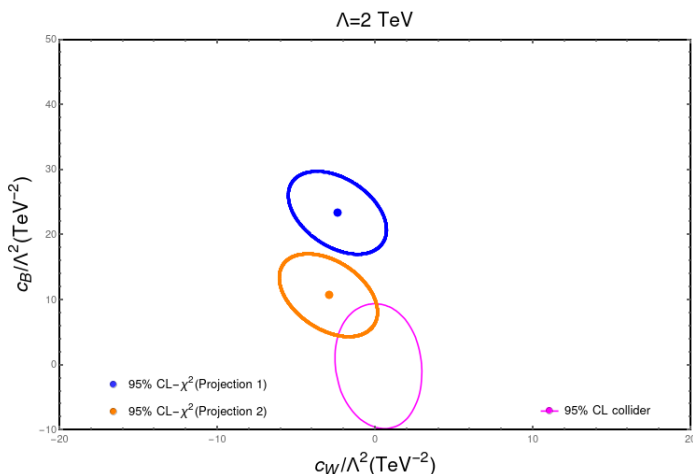


FIG. 7: The χ^2 -fit and the collider result at 95% confidence level for $\Lambda = 2$ TeV in the c_W/Λ^2 - c_B/Λ^2 plane: (a) (blue) assuming same deviations as of BMW result and corresponding errors reduced by a factor of 4 and (b) (orange) assuming no deviations from the SM result and errors reduced by a factor of 4.

2. Reduced uncertainties in Δa_μ with a vanishing central value

In the other hypothetical case of a vanishing discrepancy by the end of the FNAL run, we would have $\Delta a_\mu = 0 \pm (17.15) \times 10^{-11}$, and Fig.7(orange curve) shows the corresponding global fit. The best-fit point would

now shift by a significant amount towards the SM point with the contour ellipse having shrunk as in the preceding case. Furthermore, the best-fit ellipse now has a small overlap with the LHC contour. This fitting, thus, gives a true measure of the pull exerted by the cohort of low-energy flavour-universal observables (other than Δa_μ).

Note that the preceding projections correspond specifically to $\Lambda = 2$ TeV. For higher cutoff scales, the best fits would shift considerably towards the SM point, as had been indicated in Fig. 6b, and would offer a better reconciliation with the LHC limits as well. However, any claim about this indicating a resolution of the discrepancies through the WCs residing in the overlap are fraught with danger. For one, were hypothetical resonances that generate these WCs interacting only weakly with each other and with the SM sector, one would expect $\mathcal{O}(g_{SM}^2/16\pi^2) \lesssim (|c_B|, |c_W|) \lesssim \mathcal{O}(1)$ [31, 81], with g_{SM} denoting a typical SM coupling. However, much of the overlap region would most probably correspond to $(|c_B|, |c_W|) > \mathcal{O}(1)$ indicating a strongly interacting sector that calls into question the very method of calculating quantum corrections that we have adopted. In particular, no definite conclusion with regards to the matching of the SMEFT operators with a UV theory can be drawn.

V. SUMMARY AND OUTLOOK

Our study indicates that the limits on low-energy observables, taken individually, lead to weak bounds on the bosonic SMEFT Wilson coefficients when compared with the existing LHC limits, except for the bounds on c_W/Λ^2 emanating from the limits on ΔC_{10} which are comparable and consistent with the collider results. On the other hand, a global fit in the $(c_W/\Lambda^2, c_B/\Lambda^2)$ plane, while imposing significantly stronger constraints on the WCs,

exhibits disagreement with the LHC results. The naive expectation is that this disagreement would reduce with a (speculative) lowering of the a_μ tension in the future; on the other hand, improvements in the collider limits on the WCs are as likely to maintain the disagreement. At this juncture a cautionary remark ought to be underscored to aid our judgement. The LHC limits have used cross-sections that also include terms quadratic in the TGCs, whereas we consider contributions to the concerned observables only upto a linear order in the same. Had we included quadratic contributions, we would have obtained stronger bounds as well. Thus, in view of this caveat, it would be rash to rule out completely the scenario wherein anomalous TGCs embody some of the most dominant new physics effects addressing all of the aforementioned anomalies.

Notwithstanding the caveats, the fact that ΔC_{10} also favours c_W/Λ^2 values that are very close to the origin indicates that any explicit new physics model designed to explain the discrepancies (e.g., models which give rise to lepton flavour universality violating (LFUV) or a combination of LFUV and LFU 4-fermion operators¹¹) should either induce \mathcal{O}_W with a suppressed (or vanishing) Wil-

son coefficient or, otherwise, one must account for the WC c_W generated therein, in addition to other parameters, while performing a fit to the concerned observables. This is a crucial outcome of our study, to be regarded as a check on the existing models concerning low-energy observables, as well as a note to the model builders developing new scenarios along this line.

ACKNOWLEDGMENTS

We thank Martin Hoferichter and Diego Guadagnoli for insightful comments and for bringing to our notice some important references. K.D. acknowledges Council for Scientific and Industrial Research (CSIR), India for JRF/SRF fellowship with the award letter no. 09/045(1654)/2019-EMR-I. S.M. acknowledges research Grant No. CRG/2018/004889 of the SERB, India. L.K.S. acknowledges the UGC SRF fellowship and research Grant No. CRG/2018/004889 of the SERB, India, for partial financial support.

-
- [1] M. Du, J. Liang, Z. Liu, and V. Q. Tran, (2021), [arXiv:2104.05685 \[hep-ph\]](#).
- [2] K. Ban, Y. Jho, Y. Kwon, S. C. Park, S. Park, and P.-Y. Tseng, (2021), [arXiv:2104.06656 \[hep-ph\]](#).
- [3] L. Darmé, M. Fedele, K. Kowalska, and E. M. Sessolo, (2021), [arXiv:2106.12582 \[hep-ph\]](#).
- [4] B. Bhattacharya, A. Datta, D. Marfatia, S. Nandi, and J. Waite, (2021), [arXiv:2104.03947 \[hep-ph\]](#).
- [5] T. Nomura and H. Okada, (2021), [arXiv:2104.03248 \[hep-ph\]](#).
- [6] D. Zhang, (2021), [arXiv:2105.08670 \[hep-ph\]](#).
- [7] D. Borah, M. Dutta, S. Mahapatra, and N. Sahu, *Phys. Rev. D* **105**, 015029 (2022), [arXiv:2109.02699 \[hep-ph\]](#).
- [8] G. Arcadi, A. S. De Jesus, T. B. De Melo, F. S. Queiroz, and Y. S. Villamizar, (2021), [arXiv:2104.04456 \[hep-ph\]](#).
- [9] Y. Bai and J. Berger, (2021), [arXiv:2104.03301 \[hep-ph\]](#).
- [10] D. Choudhury, S. Maharana, D. Sachdeva, and V. Sahdev, *Phys. Rev. D* **103**, 015006 (2021), [arXiv:2007.08205 \[hep-ph\]](#).
- [11] D. Borah, M. Dutta, S. Mahapatra, and N. Sahu, *Phys. Lett. B* **820**, 136577 (2021), [arXiv:2104.05656 \[hep-ph\]](#).
- [12] M. Abdughani, Y.-Z. Fan, L. Feng, Y.-L. Sming Tsai, L. Wu, and Q. Yuan, (2021), [arXiv:2104.03274 \[hep-ph\]](#).
- [13] K. S. Babu, S. Jana, M. Lindner, and V. P. K, (2021), [arXiv:2104.03291 \[hep-ph\]](#).
- [14] W.-Y. Keung, D. Marfatia, and P.-Y. Tseng, (2021), [arXiv:2104.03341 \[hep-ph\]](#).
- [15] D. W. P. Amaral, D. G. Cerdeño, A. Cheek, and P. Foldenauer, (2021), [arXiv:2104.03297 \[hep-ph\]](#).
- [16] D. Choudhury, A. Kundu, R. Mandal, and R. Sinha, *Nucl. Phys. B* **933**, 433 (2018), [arXiv:1712.01593 \[hep-ph\]](#).
- [17] Z. Altın, O. Özdal, and C. S. Un, *Phys. Rev. D* **97**, 055007 (2018), [arXiv:1703.00229 \[hep-ph\]](#).
- [18] D. Choudhury and D. Sachdeva, *Phys. Rev. D* **100**, 075007 (2019), [arXiv:1906.06364 \[hep-ph\]](#).
- [19] W. Altmannshofer, P. S. B. Dev, A. Soni, and Y. Sui, *Phys. Rev. D* **102**, 015031 (2020), [arXiv:2002.12910 \[hep-ph\]](#).
- [20] D. Choudhury, K. Deka, and N. Kumar, *Phys. Rev. D* **104**, 035004 (2021), [arXiv:2103.10655 \[hep-ph\]](#).
- [21] J. Cao, J. Lian, Y. Pan, D. Zhang, and P. Zhu, *JHEP* **09**, 175 (2021), [arXiv:2104.03284 \[hep-ph\]](#).
- [22] W. Ke and P. Slavich, (2021), [arXiv:2109.15277 \[hep-ph\]](#).
- [23] J. S. Kim, D. E. Lopez-Fogliani, A. D. Perez, and R. R. de Austri, *Nucl. Phys. B* **974**, 115637 (2022), [arXiv:2107.02285 \[hep-ph\]](#).
- [24] A. Falkowski, M. Gonzalez-Alonso, A. Greljo, D. Marzocca, and M. Son, *JHEP* **02**, 115 (2017), [arXiv:1609.06312 \[hep-ph\]](#).
- [25] D. Choudhury, K. Deka, T. Mandal, and S. Sadhukhan, *JHEP* **06**, 111 (2020), [arXiv:2002.02349 \[hep-ph\]](#).
- [26] D. Buttazzo and P. Paradisi, (2020), [arXiv:2012.02769 \[hep-ph\]](#).
- [27] J. Aebischer, W. Dekens, E. E. Jenkins, A. V. Manohar, D. Sengupta, and P. Stoffer, (2021), [arXiv:2102.08954 \[hep-ph\]](#).
- [28] W. Buchmüller and D. Wyler, *Nuclear Physics B* **268**, 621 (1986).
- [29] B. Grzadkowski, M. Iskrzynski, M. Misiak, and J. Rosiek, *JHEP* **10**, 085 (2010), [arXiv:1008.4884 \[hep-ph\]](#).
- [30] K. Hagiwara, S. Ishihara, R. Szalapski, and D. Zeppen-

¹¹ See [82] for a review.

- feld, *Phys. Rev. D* **48**, 2182 (1993).
- [31] G. F. Giudice, C. Grojean, A. Pomarol, and R. Rattazzi, *JHEP* **06**, 045 (2007), arXiv:hep-ph/0703164.
- [32] A. Falkowski, M. González-Alonso, and K. Mimouni, *JHEP* **08**, 123 (2017), arXiv:1706.03783 [hep-ph].
- [33] H. E. Faham, F. Maltoni, K. Mimasu, and M. Zaro, (2021), arXiv:2111.03080 [hep-ph].
- [34] R. Bellan *et al.*, (2021), arXiv:2108.03199 [hep-ph].
- [35] W. Yin, *JHEP* **06**, 029 (2021), arXiv:2104.03259 [hep-ph].
- [36] J. J. Ethier, G. Magni, F. Maltoni, L. Mantani, E. R. Nocera, J. Rojo, E. Slade, E. Vryonidou, and C. Zhang (SMEFiT), *JHEP* **11**, 089 (2021), arXiv:2105.00006 [hep-ph].
- [37] G. Aad *et al.* (ATLAS), *JHEP* **11**, 005 (2020), [Erratum: *JHEP* **04**, 142 (2021)], arXiv:2006.12946 [hep-ex].
- [38] B. Abi *et al.* (Muon g-2), *Phys. Rev. Lett.* **126**, 141801 (2021), arXiv:2104.03281 [hep-ex].
- [39] T. Aoyama *et al.*, *Phys. Rept.* **887**, 1 (2020), arXiv:2006.04822 [hep-ph]; M. Davier, A. Hoecker, B. Malaescu, and Z. Zhang, *Eur. Phys. J.* **C77**, 827 (2017), arXiv:1706.09436 [hep-ph]; A. Keshavarzi, D. Nomura, and T. Teubner, *Phys. Rev.* **D97**, 114025 (2018), arXiv:1802.02995 [hep-ph]; G. Colangelo, M. Hoferichter, and P. Stoffer, *JHEP* **02**, 006 (2019), arXiv:1810.00007 [hep-ph]; M. Hoferichter, B.-L. Hoid, and B. Kubis, *JHEP* **08**, 137 (2019), arXiv:1907.01556 [hep-ph]; M. Davier, A. Hoecker, B. Malaescu, and Z. Zhang, *Eur. Phys. J.* **C80**, 241 (2020), [Erratum: *Eur. Phys. J.* **C80**, 410 (2020)], arXiv:1908.00921 [hep-ph]; A. Keshavarzi, D. Nomura, and T. Teubner, *Phys. Rev.* **D101**, 014029 (2020), arXiv:1911.00367 [hep-ph]; A. Kurz, T. Liu, P. Marquard, and M. Steinhauser, *Phys. Lett.* **B734**, 144 (2014), arXiv:1403.6400 [hep-ph]; B. Chakraborty *et al.* (Fermilab Lattice, LATTICE-HPQCD, MILC), *Phys. Rev. Lett.* **120**, 152001 (2018), arXiv:1710.11212 [hep-lat]; S. Borsanyi *et al.* (Budapest-Marseille-Wuppertal), *Phys. Rev. Lett.* **121**, 022002 (2018), arXiv:1711.04980 [hep-lat]; T. Blum, P. A. Boyle, V. Gülpers, T. Izubuchi, L. Jin, C. Jung, A. Jüttner, C. Lehner, A. Portelli, and J. T. Tsang (RBC, UKQCD), *Phys. Rev. Lett.* **121**, 022003 (2018), arXiv:1801.07224 [hep-lat]; D. Giusti, V. Lubicz, G. Martinelli, F. Sanfilippo, and S. Simula (ETM), *Phys. Rev.* **D99**, 114502 (2019), arXiv:1901.10462 [hep-lat]; E. Shintani and Y. Kuramashi, *Phys. Rev.* **D100**, 034517 (2019), arXiv:1902.00885 [hep-lat]; C. T. H. Davies *et al.* (Fermilab Lattice, LATTICE-HPQCD, MILC), *Phys. Rev.* **D101**, 034512 (2020), arXiv:1902.04223 [hep-lat]; A. Gérardin, M. Cè, G. von Hippel, B. Hörz, H. B. Meyer, D. Mohler, K. Ottnad, J. Wilhelm, and H. Wittig, *Phys. Rev.* **D100**, 014510 (2019), arXiv:1904.03120 [hep-lat]; C. Aubin, T. Blum, C. Tu, M. Golterman, C. Jung, and S. Peris, *Phys. Rev.* **D101**, 014503 (2020), arXiv:1905.09307 [hep-lat]; D. Giusti and S. Simula, *PoS LATTICE2019*, 104 (2019), arXiv:1910.03874 [hep-lat]; K. Melnikov and A. Vainshtein, *Phys. Rev.* **D70**, 113006 (2004), arXiv:hep-ph/0312226 [hep-ph]; P. Masjuan and P. Sánchez-Puertas, *Phys. Rev.* **D95**, 054026 (2017), arXiv:1701.05829 [hep-ph]; G. Colangelo, M. Hoferichter, M. Procura, and P. Stoffer, *JHEP* **04**, 161 (2017), arXiv:1702.07347 [hep-ph]; M. Hoferichter, B.-L. Hoid, B. Kubis, S. Leupold, and S. P. Schneider, *JHEP* **10**, 141 (2018), arXiv:1808.04823 [hep-ph]; A. Gérardin, H. B. Meyer, and A. Nyffeler, *Phys. Rev.* **D100**, 034520 (2019), arXiv:1903.09471 [hep-lat]; J. Bijnens, N. Hermansson-Truedsson, and A. Rodríguez-Sánchez, *Phys. Lett.* **B798**, 134994 (2019), arXiv:1908.03331 [hep-ph]; G. Colangelo, F. Hagelstein, M. Hoferichter, L. Laub, and P. Stoffer, *JHEP* **03**, 101 (2020), arXiv:1910.13432 [hep-ph]; V. Pauk and M. Vanderhaeghen, *Eur. Phys. J.* **C74**, 3008 (2014), arXiv:1401.0832 [hep-ph]; I. Danilkin and M. Vanderhaeghen, *Phys. Rev.* **D95**, 014019 (2017), arXiv:1611.04646 [hep-ph]; F. Jegerlehner, *Springer Tracts Mod. Phys.* **274**, 1 (2017); M. Knecht, S. Narison, A. Rabemananjara, and D. Rabetiarivony, *Phys. Lett.* **B787**, 111 (2018), arXiv:1808.03848 [hep-ph]; G. Eichmann, C. S. Fischer, and R. Williams, *Phys. Rev.* **D101**, 054015 (2020), arXiv:1910.06795 [hep-ph]; P. Roig and P. Sánchez-Puertas, *Phys. Rev.* **D101**, 074019 (2020), arXiv:1910.02881 [hep-ph]; G. Colangelo, M. Hoferichter, A. Nyffeler, M. Passera, and P. Stoffer, *Phys. Lett.* **B735**, 90 (2014), arXiv:1403.7512 [hep-ph]; T. Blum, N. Christ, M. Hayakawa, T. Izubuchi, L. Jin, C. Jung, and C. Lehner, *Phys. Rev. Lett.* **124**, 132002 (2020), arXiv:1911.08123 [hep-lat]; T. Aoyama, M. Hayakawa, T. Kinoshita, and M. Nio, *Phys. Rev. Lett.* **109**, 111808 (2012), arXiv:1205.5370 [hep-ph]; T. Aoyama, T. Kinoshita, and M. Nio, *Atoms* **7**, 28 (2019); A. Czarnecki, W. J. Marciano, and A. Vainshtein, *Phys. Rev.* **D67**, 073006 (2003), [Erratum: *Phys. Rev.* **D73**, 119901 (2006)], arXiv:hep-ph/0212229 [hep-ph]; C. Gnendiger, D. Stöckinger, and H. Stöckinger-Kim, *Phys. Rev.* **D88**, 053005 (2013), arXiv:1306.5546 [hep-ph].
- [40] S. Borsanyi *et al.*, *Nature* **593**, 51 (2021), arXiv:2002.12347 [hep-lat].
- [41] A. Crivellin, M. Hoferichter, C. A. Manzari, and M. Montull, *Phys. Rev. Lett.* **125**, 091801 (2020), arXiv:2003.04886 [hep-ph].
- [42] A. Keshavarzi, W. J. Marciano, M. Passera, and A. Sirlin, *Phys. Rev. D* **102**, 033002 (2020), arXiv:2006.12666 [hep-ph].
- [43] G. Colangelo, M. Hoferichter, and P. Stoffer, *Phys. Lett. B* **814**, 136073 (2021), arXiv:2010.07943 [hep-ph].
- [44] A. Keshavarzi, K. S. Khaw, and T. Yoshioka, (2021), arXiv:2106.06723 [hep-ex].
- [45] A. Gérardin, *Eur. Phys. J. A* **57**, 116 (2021), arXiv:2012.03931 [hep-lat].
- [46] A. Keshavarzi, *PoS CD2018*, 070 (2019), arXiv:1903.10349 [hep-ex].
- [47] R. Aaij *et al.* (LHCb), (2021), arXiv:2103.11769 [hep-ex].
- [48] R. Aaij *et al.* (LHCb), *Phys. Rev. Lett.* **122**, 191801 (2019), arXiv:1903.09252 [hep-ex].
- [49] R. Aaij *et al.* (LHCb), (2021), arXiv:2108.09283 [hep-ex].
- [50] C. P. Burgess, S. Godfrey, H. Konig, D. London, and I. Maksymyk, *Phys. Rev. D* **50**, 7011 (1994), arXiv:hep-ph/9307223.
- [51] B. A. Arbuzov and I. V. Zaitsev, (2021), arXiv:2105.00903 [hep-ph].
- [52] A. M. Sirunyan *et al.* (CMS), *JHEP* **12**, 062 (2019), arXiv:1907.08354 [hep-ex].
- [53] A. M. Sirunyan *et al.* (CMS), *Phys. Rev. D* **102**, 092001 (2020), arXiv:2009.00119 [hep-ex].
- [54] M. Aaboud *et al.* (ATLAS), *Eur. Phys. J. C* **79**, 884 (2019), arXiv:1905.04242 [hep-ex].
- [55] S. Chang, J. Hisano, H. Nakano, N. Okada, and M. Yamaguchi, *Phys. Rev. D* **62**, 084025 (2000), arXiv:hep-

- ph/9912498.
- [56] C. Csaki, J. Erlich, and J. Terning, *Phys. Rev. D* **66**, 064021 (2002), [arXiv:hep-ph/0203034](#).
- [57] K. Agashe, A. Delgado, M. J. May, and R. Sundrum, *JHEP* **08**, 050 (2003), [arXiv:hep-ph/0308036](#).
- [58] M. T. Arun and D. Choudhury, *JHEP* **09**, 202 (2015), [arXiv:1501.06118 \[hep-th\]](#).
- [59] M. T. Arun and D. Choudhury, *JHEP* **04**, 133 (2016), [arXiv:1601.02321 \[hep-ph\]](#).
- [60] K. S. Babu, S. Nandi, and Z. Tavartkiladze, *Phys. Rev. D* **80**, 071702 (2009), [arXiv:0905.2710 \[hep-ph\]](#); F. Bonnet, D. Hernandez, T. Ota, and W. Winter, *JHEP* **10**, 076 (2009), [arXiv:0907.3143 \[hep-ph\]](#); T. Li and X.-G. He, *Phys. Rev. D* **80**, 093003 (2009), [arXiv:0907.4193 \[hep-ph\]](#); I. Picek and B. Radovic, *Phys. Lett. B* **687**, 338 (2010), [arXiv:0911.1374 \[hep-ph\]](#); Y. Liao, *Phys. Lett. B* **694**, 346 (2011), [arXiv:1009.1692 \[hep-ph\]](#); A. Delgado, C. Garcia Cely, T. Han, and Z. Wang, *Phys. Rev. D* **84**, 073007 (2011), [arXiv:1105.5417 \[hep-ph\]](#); K. Kumericki, I. Picek, and B. Radovic, *Phys. Rev. D* **84**, 093002 (2011), [arXiv:1106.1069 \[hep-ph\]](#); F. Bonnet, M. Hirsch, T. Ota, and W. Winter, *JHEP* **07**, 153 (2012), [arXiv:1204.5862 \[hep-ph\]](#); K. Kumericki, I. Picek, and B. Radovic, *Phys. Rev. D* **86**, 013006 (2012), [arXiv:1204.6599 \[hep-ph\]](#); T. Ma, B. Zhang, and G. Cacciapaglia, *Phys. Rev. D* **89**, 015020 (2014), [arXiv:1309.7396 \[hep-ph\]](#); K. L. McDonald, *JHEP* **11**, 131 (2013), [arXiv:1310.0609 \[hep-ph\]](#); T. Ma, B. Zhang, and G. Cacciapaglia, *Phys. Rev. D* **89**, 093022 (2014), [arXiv:1404.2375 \[hep-ph\]](#); Y. Yu, C.-X. Yue, and S. Yang, *Phys. Rev. D* **91**, 093003 (2015), [arXiv:1502.02801 \[hep-ph\]](#); P. Ko and T. Nomura, *Phys. Lett. B* **753**, 612 (2016), [arXiv:1510.07872 \[hep-ph\]](#); R. Cepedello, M. Hirsch, and J. C. Helo, *JHEP* **01**, 009 (2018), [arXiv:1709.03397 \[hep-ph\]](#); G. Anamiati, O. Castillo-Felisola, R. M. Fonseca, J. C. Helo, and M. Hirsch, *JHEP* **12**, 066 (2018), [arXiv:1806.07264 \[hep-ph\]](#); S. Kumar Agarwalla, K. Ghosh, and A. Patra, *JHEP* **05**, 123 (2018), [arXiv:1803.01670 \[hep-ph\]](#); S. K. Agarwalla, K. Ghosh, N. Kumar, and A. Patra, *JHEP* **01**, 080 (2019), [arXiv:1808.02904 \[hep-ph\]](#); C. Arbeláez, J. C. Helo, and M. Hirsch, *Phys. Rev. D* **100**, 055001 (2019), [arXiv:1906.03030 \[hep-ph\]](#); N. Kumar, T. Nomura, and H. Okada, *Eur. Phys. J. C* **80**, 801 (2020), [arXiv:1912.03990 \[hep-ph\]](#); S. Ashanujjaman and K. Ghosh, *JHEP* **06**, 084 (2021), [arXiv:2012.15609 \[hep-ph\]](#).
- [61] N. Kumar and V. Sahdev, (2021), [arXiv:2112.09451 \[hep-ph\]](#).
- [62] S. Ashanujjaman, D. Choudhury, and K. Ghosh, (2022), [arXiv:2201.09645 \[hep-ph\]](#).
- [63] G. Gounaris *et al.*, in *AGS / RHIC Users Annual Meeting* (1996) [arXiv:hep-ph/9601233](#).
- [64] A. De Rújula, M. Gavela, P. Hernandez, and E. Massó, *Nuclear Physics B* **384**, 3 (1992).
- [65] C. P. Burgess and D. London, *Phys. Rev. Lett.* **69**, 3428 (1992).
- [66] R. Alonso, E. E. Jenkins, A. V. Manohar, and M. Trott, *JHEP* **04**, 159 (2014), [arXiv:1312.2014 \[hep-ph\]](#).
- [67] C. Bobeth and U. Haisch, *JHEP* **09**, 018 (2015), [arXiv:1503.04829 \[hep-ph\]](#).
- [68] C. P. Burgess and D. London, *Phys. Rev. D* **48**, 4337 (1993), [arXiv:hep-ph/9203216](#).
- [69] A. M. Sirunyan *et al.* (CMS), *Phys. Lett. B* **772**, 21 (2017), [arXiv:1703.06095 \[hep-ex\]](#).
- [70] G. Aad *et al.* (ATLAS), *JHEP* **09**, 029 (2016), [arXiv:1603.01702 \[hep-ex\]](#).
- [71] V. Khachatryan *et al.* (CMS), *Eur. Phys. J. C* **76**, 401 (2016), [arXiv:1507.03268 \[hep-ex\]](#).
- [72] S. Schael *et al.* (ALEPH, DELPHI, L3, OPAL, LEP Electroweak), *Phys. Rept.* **532**, 119 (2013), [arXiv:1302.3415 \[hep-ex\]](#).
- [73] *Combined Higgs boson production and decay measurements with up to 137 fb⁻¹ of proton-proton collision data at $\sqrt{s} = 13$ TeV*, Tech. Rep. (CERN, Geneva, 2020).
- [74] T. Hurth, F. Mahmoudi, D. M. Santos, and S. Neshatpour, *Phys. Lett. B* **824**, 136838 (2022), [arXiv:2104.10058 \[hep-ph\]](#).
- [75] A. Carvunis, F. Dettori, S. Gangal, D. Guadagnoli, and C. Normand, *JHEP* **12**, 078 (2021), [arXiv:2102.13390 \[hep-ph\]](#).
- [76] W. Altmannshofer and P. Stangl, *Eur. Phys. J. C* **81**, 952 (2021), [arXiv:2103.13370 \[hep-ph\]](#).
- [77] M. Algueró, B. Capdevila, S. Descotes-Genon, J. Matias, and M. Novoa-Brunet (2021) [arXiv:2104.08921 \[hep-ph\]](#).
- [78] W. Altmannshofer and D. M. Straub, *Eur. Phys. J. C* **75**, 382 (2015), [arXiv:1411.3161 \[hep-ph\]](#).
- [79] A. Arbey, T. Hurth, F. Mahmoudi, and S. Neshatpour, *Phys. Rev. D* **98**, 095027 (2018), [arXiv:1806.02791 \[hep-ph\]](#).
- [80] M. Ciuchini, E. Franco, S. Mishima, and L. Silvestrini, *JHEP* **08**, 106 (2013), [arXiv:1306.4644 \[hep-ph\]](#).
- [81] D. Marzocca *et al.*, (2020), [arXiv:2009.01249 \[hep-ph\]](#).
- [82] D. London and J. Matias, (2021), 10.1146/annurev-nucl-102020-090209, [arXiv:2110.13270 \[hep-ph\]](#).